Supporting Information

Fahlke et al. 10.1073/pnas.1108927108

SI Methods

Specimens Studied. Archaeocetes included in this study represent middle Eocene Protocetidae and late Eocene Basilosauridae. Specimens were screened for damage and postmortem deformation. Taphonomically and artificially deformed specimens were omitted from the analysis. To avoid a possible influence of ontogenetic changes of cranial asymmetry on our results, we only used crania of adult individuals. Species studied are: *Artiocetus clavis* (GSP-UM 3458): complete cranium of a partial skeleton collected from the middle Eocene (47 Ma) upper Habib Rahi Formation of Balochistan Province, Pakistan (1); *Qaisracetus arifi* (GSP-UM 3316): cranium of a partial skeleton collected from the middle Eocene (43 Ma) Domanda Formation of Balochistan Province, Pakistan (2); *Dorudon atrox* (UM 101222): complete cranium collected from the late Eocene (37 Ma) Birket Qarun Formation of Wadi Al Hitan, Egypt (3); *Dorudon atrox* (SMF 4451): complete cranium collected from the late Eocene (37 Ma) Birket Qarun or Qasr el-Sagha Formation of Fayum, Egypt (4); *Basilosaurus isis* (WH-74): skull pieces, reconstructed skull cast, and left and right mandibles of a virtually complete skeleton collected from the late Eocene (37 Ma) Birket Qarun Formation of Wadi Al Hitan, Egypt. Measurements of *B. isis* (SMNS 11787, complete skull from the late Eocene Birket Qarun Formation, Fayum, Egypt) were taken from a published figure (plate VII.1 in ref. 4). Specimen numbers of the comparative modern artiodactyl sample are given in Tables S1 and S2.

Three-Dimensional Scanning and Preparation. The cranium of *A. clavis* (GSP-UM 3458) and the dentaries of *B. isis* (WH-74) were CT-scanned (GE HD-750) in the Department of Radiology at the University Hospital, University of Michigan. In-plane resolution is 0.293 to 0.742 mm for *A. clavis* and 0.879 mm for *B. isis*; slice thickness is 0.625 mm for all samples. Surface models were generated using Amira software and enhanced using Materialise 3-matic and Magics software. The skull model was reoriented in a global *x-y-z* coordinate system using a script written in R statistical programming language (5).

Micro-CT scans (GE phoenix|X-ray v|tome|x s) of the cranium of *A. clavis* were made at the Steinmann-Institut, University of Bonn, Germany. Isotropic voxel size of the scan used is $(0.198\ \text{mm})^3$.

Analysis of Midline Suture Deviation. All crania were carefully oriented and photographed in dorsal view using a long focal-length lens to minimize parallax. Deviations were measured in Adobe Photoshop. We measured the deviation, δx, of the dorsal midline suture from a straight rostrocaudal axis, RC, in one-tenth increments along RC (measurements in millimeters). RC was used as a reference axis, following Ness (6), with R being a point on the midline at the tip of the rostrum and C being a point on the midline posterior to the foramen magnum bisecting the posteriormost extent of the occipital condyles (Fig. S1). Note that RC is not equivalent to the global *x* axis in an asymmetrical skull.

In Odontoceti, the rostrum is not affected by telescoping. Thus, a similar δx at the bony nares might result in different skew values for Odontoceti with different rostrum lengths (6, 7). However, archaeocete torsion does affect the rostrum (Fig. 1*B*). Therefore, we decided not to use Ness' calculation of skew, but sampled δx at nine equally spaced points along RC (dividing RC into tenths). To make the measurements size-independent we calculated deviations relative to RC (δx/RC) (Fig. 2).

For a symmetrical comparative baseline sample we quantified natural variation in 24 artiodactyl skulls (two *Alces americana*, two *Antilocapra americana*, three *Bison bison*, one *Bos taurus*, one *Camelus bactrianus*, two *Camelus dromedarius*, five *Cervus canadensis*, one *Giraffa camelopardalis*, three *Hippopotamus amphibius*, one *Oreamnos montanus*, one *Sus cristatus,* and two *Sus scrofa*). Statistical significance was calculated following Sokal and Rohlf (8).

Analysis of Deflection Angles. We sampled coordinates of vertices along the ventral ($n = 23$) and dorsal ($n = 21$) midline sutures on the 3D skull model of *A. clavis*. Applying an R (5) script, 1,000 points, each separated by 0.57 mm along the *x* axis, were interpolated from these coordinates using a cubic spline for each suture. The deviation of a line connecting each pair of dorsal and ventral midline points from the *xz*-plane was taken as the deflection angle (Fig. 3).

Analysis of Air Sinuses. Air sinuses of *A. clavis* were reconstructed from University of Bonn micro-CT images using Amira (Fig. 1*B*).

Bone-Thickness Measurements. We measured bone thicknesses of the outer walls of both left and right dentaries of *B. isis* on a 25×25-mm grid using Amira software and University of Michigan CT images. The measurements were then used to create thickness maps in ESRI ArcGIS (Fig. 4).

1. Gingerich PD, Haq MU, Zalmout IS, Khan IH, Malkani MS (2001) Origin of whales from early artiodactyls: Hands and feet of Eocene Protocetidae from Pakistan. *Science* 293:2239–2242.
2. Gingerich PD, Haq MU, Hussain Khan I, Zalmout IS (2001) Eocene stratigraphy and archaeocete whales (Mammalia, Cetacea) of Drug Lahar in the eastern Sulaiman Range, Balochistan (Pakistan). *Contributions of the Museum of Paleontology University of Michigan* 30:269–319.
3. Uhen MD (2004) Form, function, and anatomy of *Dorudon atrox* (Mammalia, Cetacea): An archaeocete from the middle to late Eocene of Egypt. *University of Michigan Papers on Paleontology* 34:1–222.
4. Stromer E (1908) Die Archaeoceti des ägyptischen Eozäns (Archaeocetes of the Egyptian Eocene). *Beiträge zur Paläontologie und Geologie Österreich-Ungarns und des Orients, Vienna*, 21:106–178 (in German).
5. R Development Core Team (2010) R: A Language and Environment for Statistical Computing, http://www.R-project.org. Accessed June 29, 2010.
6. Ness AR (1967) A measure of asymmetry of the skulls of odontocete whales. *J Zool* 153:209–211.
7. Heyning JE (1989) Comparative facial anatomy of beaked whales (Ziphiidae) and a systematic revision among the families of extant Odontoceti. *Natural History Museum of Los Angeles County Contributions in Science* 405:1–64.
8. Sokahl RR, Rohlf FJ (1981) *Biometry* (W. H. Freeman, New York), 2nd Ed.

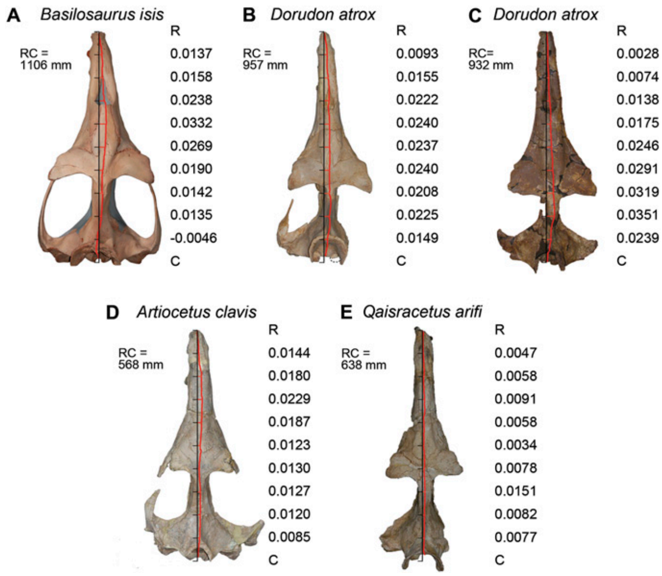

Fig. S1. Archaeocete crania studied here with relative deviations of the dorsal midline suture (δx/RC). (*A*) *B. isis* (WH-74, reconstruction made by reassembling well-preserved skull pieces), late Eocene (37 Ma), Egypt; (*B*) *D. atrox* (UM 101222), late Eocene (37 Ma), Egypt; (*C*) *D. atrox* (SMF 4451), late Eocene (37 Ma), Egypt; (*D*) *A. clavis* (GSP-UM 3458), middle Eocene (47 Ma), Pakistan; (*E*) *Q. arifi* (GSP-UM 3316) middle Eocene (43 Ma), Pakistan. All crania are shown in dorsal view, scaled to the same rostrocaudal length (RC). Red lines are the dorsal midline sutures. Note that the dorsal midline suture deviates to the right relative to RC in all crania. For dorsal view of *B. isis* (SMNS 11787, late Eocene, Egypt), see plate VII.1 in Stromer (4). All measurements, including those for SMNS 11787, are given in Tables S1 and S2.

Table S1. Relative midline suture deviations (δx/RC) for the comparative modern artiodactyl sample and the archaeocete crania studied here

Species	Specimen	δ10/RC	δ20/RC	δ30/RC	δ40/RC	δ50/RC	δ60/RC	δ70/RC	δ80/RC	δ90/RC	Mean δx/RC	Zero mean dist.
Alces americana	UM no number	−0.0017	0.0000	0.0000	−0.0024	−0.0051	−0.0042	0.0000	0.0019	0.0019	−0.0011	0.0004
Alces americana	UM R 1437	−0.0040	−0.0040	−0.0067	−0.0071	−0.0052	−0.0056	−0.0040	−0.0025	−0.0025	−0.0046	−0.0031
Antilocapra americana	UM R 1607	0.0044	0.0040	−0.0018	0.0000	−0.0018	−0.0040	−0.0080	−0.0033	−0.0033	−0.0015	0.0000
Antilocapra americana	UM R 1608	0.0000	−0.0022	−0.0089	−0.0115	−0.0115	−0.0081	−0.0044	−0.0048	−0.0048	−0.0062	−0.0047
Bison bison	UMMZ 156570	0.0013	0.0048	0.0077	0.0042	0.0038	0.0115	0.0119	0.0115	0.0038	0.0067	0.0082
Bison bison	UMMZ 30061	0.0029	−0.0130	−0.0116	−0.0086	−0.0102	−0.0049	−0.0120	0.0024	−0.0035	−0.0065	−0.0050
Bison bison	UMMZ 61294	0.0031	0.0000	0.0000	0.0000	0.0000	−0.0015	0.0031	0.0072	0.0013	0.0015	0.0030
Bos taurus	UM no number	0.0000	−0.0036	−0.0040	−0.0040	−0.0051	−0.0044	−0.0065	0.0046	0.0046	−0.0020	−0.0005
Camelus bactrianus	UMMZ 4619	0.0000	0.0000	−0.0015	−0.0036	0.0000	0.0000	0.0000	0.0040	0.0040	0.0003	0.0018
Camelus dromedarius	UM no number	0.0000	0.0000	−0.0085	−0.0028	−0.0059	−0.0074	−0.0093	−0.0066	−0.0066	−0.0052	−0.0037
Camelus dromedarius	UMMZ 122700	0.0000	0.0000	−0.0043	−0.0050	−0.0050	−0.0035	−0.0052	−0.0013	−0.0013	−0.0028	−0.0013
Cervus canadensis	UM J 59	0.0000	−0.0043	−0.0051	−0.0047	−0.0043	−0.0029	−0.0070	−0.0051	−0.0051	−0.0043	−0.0028
Cervus canadensis	UM no number	0.0000	0.0000	−0.0010	0.0048	0.0000	−0.0044	−0.0032	−0.0038	−0.0038	−0.0013	0.0002
Cervus canadensis	UMMZ 175461	0.0062	0.0115	0.0148	0.0167	0.0153	0.0139	0.0096	0.0072	0.0029	0.0109	0.0124
Cervus canadensis	UMMZ 59799	0.0000	−0.0014	0.0009	0.0030	0.0035	0.0026	0.0014	−0.0019	0.0000	0.0009	0.0024
Cervus canadensis	UMMZ 62122	0.0040	−0.0044	−0.0009	0.0009	0.0044	0.0044	0.0042	0.0000	0.0000	0.0014	0.0029
Giraffa camelopardalis	UM J 17	0.0009	0.0014	0.0014	0.0009	0.0000	0.0000	−0.0043	0.0000	0.0000	0.0000	0.0015
Hippopotamus amphibius	UMMZ 112380	−0.0062	−0.0040	−0.0052	−0.0030	−0.0023	−0.0028	−0.0013	−0.0039	−0.0039	−0.0036	−0.0021
Hippopotamus amphibius	UMMZ 112381	−0.0080	−0.0100	−0.0097	−0.0084	−0.0071	−0.0020	−0.0033	−0.0080	−0.0080	−0.0072	−0.0057
Hippopotamus amphibius	UMMZ 84041	−0.0116	−0.0116	−0.0098	−0.0111	−0.0081	−0.0197	−0.0050	−0.0026	−0.0026	−0.0091	−0.0076
Oreamnos montanus	UM R 1438	0.0027	0.0043	−0.0077	−0.0060	−0.0057	−0.0070	−0.0083	−0.0073	−0.0073	−0.0047	−0.0032
Sus cristatus	UM 52	0.0000	0.0000	0.0019	0.0055	0.0000	0.0069	0.0080	0.0025	0.0025	0.0030	0.0045
Sus scrofa	UM J 41	0.0009	0.0020	0.0046	0.0057	0.0046	0.0000	0.0000	0.0000	0.0000	0.0020	0.0035
Sus scrofa	UMMZ no number	−0.0064	−0.0064	−0.0042	0.0000	−0.0016	−0.0013	−0.0026	−0.0016	−0.0016	−0.0028	−0.0013
											SD of means 0.0045	Mean of means = 0.0000
Basilosaurus isis	WH-74	0.0137	0.0158	0.0238	0.0332	0.0269	0.0190	0.0142	0.0135	−0.0046	0.0173	
Basilosaurus isis	SMNS 11787	0.0032	−0.0011	0.0009	0.0015	0.0040	0.0038	0.0023	0.0052	0.0055	0.0028	
Dorudon atrox	UM 101222	0.0093	0.0155	0.0222	0.0240	0.0237	0.0240	0.0208	0.0225	0.0149	0.0197	
Dorudon atrox	SMF 4451	0.0028	0.0074	0.0138	0.0175	0.0246	0.0291	0.0319	0.0351	0.0239	0.0207	
Artiocetus clavis	GSP-UM 3458	0.0144	0.0180	0.0229	0.0187	0.0123	0.0130	0.0127	0.0120	0.0085	0.0147	
Qaisracetus arifi	GSP-UM 3316	0.0047	0.0058	0.0091	0.0058	0.0034	0.0078	0.0151	0.0082	0.0077	0.0075	

dist., distribution; SD, standard deviation.

Table S2. Descriptive and *t*-test statistics for the archaeocete crania studied here

			Y2: Symmetrical model artiodactyl sample			Y1: Archaeocete test sample			*t*-test worksheet			Results	
Species	Specimen	Test	*N*	Mean	SD	*N*	Mean	SD	Num	Denom1	Denom2	Student *t*	*P*
Basilosaurus isis	WH-74	1	24	0.0000	0.0045	1	0.0173	0.0000	0.0173	0.000020	1.0417	3.7419	0.0011
Basilosaurus isis	SMNS 11787	2	24	0.0000	0.0045	1	0.0028	0.0000	0.0028	0.000020	1.0417	0.6073	0.5496
Basilosaurus isis	Both two above	3	24	0.0000	0.0045	2	0.0100	0.0102	0.0100	0.000024	0.5417	2.7861	0.0103
Dorudon atrox	UM 101222	4	24	0.0000	0.0045	1	0.0197	0.0000	0.0197	0.000020	1.0417	4.2617	0.0003
Dorudon atrox	SMF 4451	5	24	0.0000	0.0045	1	0.0207	0.0000	0.0207	0.000020	1.0417	4.4825	0.0002
Dorudon atrox	Both two above	6	24	0.0000	0.0045	2	0.0202	0.0007	0.0202	0.000020	0.5417	6.1900	0.0000
Artiocetus clavis	GSP-UM 3458	7	24	0.0000	0.0045	1	0.0147	0.0000	0.0147	0.000020	1.0417	3.1886	0.0041
Qaisracetus arifi	GSP-UM 3316	8	24	0.0000	0.0045	1	0.0075	0.0000	0.0075	0.000020	1.0417	1.6272	0.1173
All archaeocetes	All six above	9	24	0.0000	0.0045	6	0.0138	0.0071	0.0138	0.000026	0.2083	5.9289	0.0000

Note that all archaeocete midline sutures deviate to the right (orange), the six archaeocetes as a group deviate significantly more than expected for a symmetrical sample, and four of the six individual archaeocete crania deviate significantly more than expected for a symmetrical sample. Yellow-cell *t* values are significant at $P < 0.05$. Blue-cell *t* values are not significant. Denom, denominator; *N*, sample size; Num, numerator; *P*, probability; *SD*, standard deviation.